C. R. Mecanique 343 (2015) 612–621

Contents lists available at ScienceDirect

Comptes Rendus Mecanique

www.sciencedirect.com

Acoustic metamaterials and phononic crystals

Effective birefringence to analyze sound transmission through a layer with subwavelength slits

Étude de la transmission du son par une lame perforée de trous sub-longueur d'onde

Agnès Maurel [a,*], Simon Félix [b], Jean-François Mercier [c], Abdel Ourir [a]

[a] *Institut Langevin, CNRS, ESPCI ParisTech, 1, rue Jussieu, 75005 Paris, France*
[b] *LAUM, CNRS, Université du Maine, avenue Olivier-Messiaen, 72085 Le Mans, France*
[c] *Poems, CNRS, ENSTA ParisTech, INRIA, 828, boulevard des Maréchaux, 91762 Palaiseau, France*

ARTICLE INFO

Article history:
Received 17 January 2015
Accepted 10 July 2015
Available online 5 August 2015

Keywords:
Metamaterial
Spoof plasmon
Homogenization
Acoustic array

Mots-clés :
Métamatériau
Spoof plasmon
Homogénéisation
Réseau acoustique

ABSTRACT

We analyze the transmission of sound through a sound hard film or layer with periodic subwavelength slits. For wavelength comparable to or larger than the slit spacing, the transmission spectra are revisited in terms of the transmission through an equivalent birefringent layer. It is shown that the Fano-type resonances can be understood by means of the dispersion relations of guided waves within the birefringent layer in the homogenized problem, equivalent to spoof plasmons for gratings. This is done by extending the homogenization to the evanescent waves being excited in the near field of the actual perforated layer.

RÉSUMÉ

Nous analysons les spectres de transmission par une lame rigide perforée périodiquement de trous sub-longueur d'onde. Pour des longueurs d'onde comparables ou plus grandes que l'espacement des perforations, les spectres de transmission sont revisités en termes de transmission par une lame équivalente biréfringente. Nous montrons que les résonances de Fano se comprennent au vu des relations de dispersion d'ondes guidées par la couche biréfringente, similaires aux *spoof plasmons* dans les réseaux en réflexion. Ces relations de dispersion sont obtenues en étendant l'homogénéisation aux ondes évanescentes excitées en champ proche dans le problème réel.

Version française abrégée

En 1902, Wood rend compte d'un phénomène qu'il considère comme le plus intéressant qu'il ait jamais rencontré : l'extinction totale et soudaine de luminosité dans le spectre de réflexion d'un réseau optique [1]. Ce faisant, il ouvre la

* Corresponding author.
E-mail addresses: agnes.maurel@espci.fr (A. Maurel), simon.felix@univ-lemans.fr (S. Félix), mercier@ensta.fr (J.-F. Mercier), aourir@espci.fr (A. Ourir).

http://dx.doi.org/10.1016/j.crme.2015.07.006
1631-0721/

voie à ce qui est devenu depuis plusieurs années la « plasmonique », avec la découverte d'ondes de surface (*surface plasmon polaritons*) qui peuvent se propager à la surface d'un métal dans l'infrarouge et d'ondes guidées (*spoof splasmons*) qui se propagent dans des guides structurés. En acoustique, les plasmons de surface ne peuvent pas exister, car cela supposerait un milieu de masse volumique négative, ce qui est peu commun. En revanche, les *spoof plasmons* (qui miment les plasmons) correspondent à des ondes guidées dans des guides structurés alternant un matériau lourd et de l'air, avec des conditions de Neumann pour le matériau lourd. Leur relation de dispersion a été calculée dans le contexte des ondes acoustiques en 1997 [8], et ils ont été popularisés dans le domaine des ondes électromagnétiques en 2005 comme une alternative aux plasmons de surface dans l'infrarouge lointain [5]. Dans ces deux études, le calcul s'appuie sur une analyse des ondes dans les sillons d'air d'un réseau. Dans la Réf. [5], les auteurs remarquent que la couche structurée se comporte comme un milieu homogène anisotrope. Nous avons montré que la théorie d'homogénéisation des milieux en couche permet de retrouver directement ce résultat [16] en considérant la limite Neumann d'une masse volumique et d'un module d'élasticité infinis. Dans ces approches, monomodales ou homogénéisées, on suppose que la longueur d'onde est très grande devant les dimensions de la microstructure, c'est-à-dire le régime des basses fréquences.

Dans ce papier, nous nous intéressons à la transmission du son à travers une couche massive (*sound hard*) perforée de trous dans des régimes de fréquences basses et intermédiaires (Fig. 1, avec $w/h = 0.1$). Pour ce faire, nous utilisons la théorie de l'homogénéisation, qui permet de remplacer la couche perforée par une couche homogène biréfringente, dont le spectre de transmission est aisé à calculer (Eq. (9)). Dans le problème homogénéisé classique (Eqs. (3)–(10)), on s'attend à une transmission parfaite $|T| = 1$ dans deux cas (Eq. (10)), qui correspondent respectivement à (i) une condition de raccord d'impédances entre l'air et la couche biréfringente et à (ii) une condition de résonance de Fabry–Pérot (FP). Dans le régime basses fréquences, l'expression du champ de pression p issue du problème homogénéisé (Eq. (7)), constitue une excellente approximation du champ de pression exact p^{ex} pour la condition (i), non résonante, mais elle est une approximation raisonnable seulement pour la condition résonante de FP (ii), Figs. 2 et 3 (p^{ex} est calculé numériquement par une méthode modale qui résout le problème exact (Eq. (1)) [13]. Pour comprendre ce désaccord, on inspecte les spectres de transmission dans le plan (θ, kh) pour une épaisseur de couche $\ell = 0.3h$ et dans le plan $(\ell/h, kh)$ pour une incidence normale $\theta = 0$ (Fig. 4). Dans les deux cas, $kh < 4\pi$ couvre des régimes de fréquences intermédiaires pour lesquelles jusqu'à quatre ondes peuvent devenir propagatives (au-dessus de leurs fréquences de coupure k_n^{c}, données par les Eqs. (2)). Comme attendu, le spectre homogénéisé ne rend pas compte de la complexité de T^{ex} dès lors que la première fréquence de coupure est dépassée. Notamment, à chaque coupure, l'onde incidente s'éteint complètement en transmission (DR sur la Fig. 5) ; ces phénomènes sont les équivalents, pour notre réseau en transmission, des extinctions observées par Wood pour un réseau en réflexion. Nous les qualifions de résonances destructives (DR), puisqu'elles correspondent à des résonances (de type guide d'onde) qui affaiblissent la transmission de l'onde incidente. Il est bien sûr impossible de les retrouver dans notre résultat homogénéisé, puisqu'en supposant $k \to 0$, on renvoie la première coupure à l'infini. Mais, de façon plus intéressante, on constate des maxima locaux de la transmission, qui sont décalés plus ou moins nettement des FP prévus par l'homogénéisation, y compris dans le régime basse fréquence (CR sur la Fig. 5).

Ces variations dans le spectre, qui peuvent être brutales, traduisent une interaction de l'onde incidente avec des ondes excitées dans le champ proche de la couche perforée, et qui sont visibles dans les champs de pression p^{ex} de la Fig. 3 au voisinage de $x = \ell$. Pour expliquer ces comportements, nous retournons vers le modèle homogénéisé, mais en considérant cette fois une onde incidente évanescente (Eq. (12)). Le formalisme est le même, mais nous cherchons maintenant une condition de résonance, c'est-à-dire une divergence des coefficients R_n et T_n (Eq. (13)). Nous déterminons ainsi la relation de dispersion des ondes guidées dans la couche biréfringente (Eq. (15)), c'est-à-dire d'une onde résonante dans la couche et évanescente dans l'air. Les courbes de dispersion obtenues sont reportées sur les spectres de T^{ex} sur la Fig. 6 : on observe que les augmentations de la transmission de l'onde incidente coïncident raisonnablement avec les résonances des modes évanescents prévus par homogénéisation, et ce bien au-delà des basses fréquences (nous les qualifions donc de résonances constructives, CR).

Pour vérifier que ces modes guidés du problème homogénéisé ont un lien avec la physique de la couche perforée, nous considérons les deux points suivants. Tout d'abord, nous revenons au cas des transmissions parfaites considérées sur la Fig. 3, et qui étaient décalées par rapport à la première prédiction des résonances de FP. Sur la Fig. 7, sur les champs de pression exacts p^{ex}, on montre dans les inserts les champs de pression p_1 des modes guidés dans le problème homogénéisé, révélant un bon accord qualitatif. Finalement, la Fig. 8 donne les coefficients de réflexion T_n^{ex} des ondes évanescentes calculés numériquement (Eq. (1)), mais en ne considérant que l'onde incidente et une onde évanescente. De grandes valeurs de $|T_n^{\text{ex}}|$ sont effectivement atteintes, qui traduisent des résonances d'ondes évanescentes dans le problème exact, très bien décrites par les résonances des modes guidés dans le problème homogénéisé.

Nous concluons que l'homogénéisation peut expliquer finement les variations de transmission d'une couche ou d'un réseau structuré. Au-delà de l'homogénéisation classique, qui considère seulement le champ de pression incident, les résonances d'ondes évanescentes associées à des ondes guidées dans la couche homogénéisée pilotent les variations observées dans le spectre réel. De façon prospective, la Fig. 10 rapporte les spectres en transmission calculés numériquement en ne prenant en compte que l'onde incidente et la première onde à passer sa coupure, améliorant significativement la validité du calcul. Il semble donc possible de développer un modèle homogénéisé à deux ondes, et nous travaillons dans cette direction.

1. Introduction

In 1902, Wood observed sudden extinctions in the reflection spectrum given by an optical metallic grating [1], and these phenomena, later interpreted partially by Rayleigh [2] and in more deep details by Hessel and Oliner [3], have kept the name of "anomalies" given by Wood, who considered them as "one of the most interesting that [he has] ever met with". Much more recently, there has been a huge interest in the plasmon polaritons, spoof plasmons and other re-baptized surface and guided waves but, as indicated by Maystre in this review "let us give back to Caesar what is Caesar's: Wood must be considered as the initiator of plasmonics" [4].

Surface plasmons are resonant surface waves being trapped at the interface between a dielectric medium and a metal in the visible range, that is with negative permeability. These surface waves cannot exist in the context of acoustic waves, where negative mass density and unitary bulk modulus are, to say the least, not usual. Spoof plasmons have been proposed by Garcia-Vidal, Martín-Moreno and Pendry in 2005 as an alternative to surface plasmons able to exist in the far infrared [5]; these are guided waves within a structured guide. In this range of frequencies, common metals behave as "wave hard" material, with a high permeability, hence a high impedance mismatch. For two-dimensional structures and transverse magnetic polarization of the waves, this is equivalent to a Neumann boundary condition. Wave hard materials are the most common materials in the context of sound waves, and this analogy has attracted a serious interest in the community of acoustics, where spoof plasmons in structured waveguides have revealed interesting phenomena, as the rainbow effect obtained with a one-dimensional structuring of the guide [6] or wave propagation control at sub-wavelength scales obtained with a two-dimensional structuring [7]. Note that the dispersion relation of acoustic spoof plasmons was derived by Kelders, Allard and Lauriks in 1997 [8]; these authors called them surface waves, which is possibly not a proper term neither.

The virtue of these guided waves is linked to their resonant behavior, able to enhance or to forbid the transmission through arrays. This implies energy exchange between the incident wave and the guided wave: to come back to Wood's observations, anomalies are associated with a new interference order, that is a grazing wave becoming propagating just above its cut-off frequency, and which takes all the energy from the incident wave. Being grazing along the grating, it does not let any trace on the reflection spectrum (its energy is sent to infinity rather than on the observation screen), leading to an apparent complete extinction.

The problem is simpler in acoustics that in electromagnetism in two ways. First, the analogy between one- and two-dimensional structures is less hazardous in the context of acoustics since the Neumann boundary condition is not subjected to a particular polarization of the wave (the transverse magnetic polarization, the transverse electric polarization leading to Dirichlet boundary condition). Next, for two-dimensional structures, it is straightforward to use the homogenization theory that offers a simplified and rigorous mathematical formulation of the problem. Again, this is much simpler in the context of acoustics since the Neumann limit is associated with infinite impedance ratio but finite wavelength (both mass density and bulk modulus being large but of the same order of magnitude), while in the context of electromagnetism, only the permeability becomes large, leading to vanishing wavelength, which is not compatible with the homogenization limit [9,10]. This has probably limited the use of rigorous homogenization for perfectly conducting metals, and other approaches have been retained, among which an empirical isotropic homogenization [11] or the use of approximate modal expansions to retrieve the anisotropic effective parameters [5,12].

In this paper, we study the transmission spectra of a sound hard film or layer perforated with thin slits. This is done by considering the analog homogeneous but birefringent film or layer obtained with the classical homogenization theory of layered media, which preserves the anisotropy of the actual structured material. Homogenization is justified for an infinite medium while a film or a layer has a finite thickness ℓ; it has already been shown that ℓ does not need to be large nor small to get accurate results [16]. Nevertheless, the periodicity h of the actual structure being lost in the homogenization process, the wavelength has to be large compared to h in order to argue that the wave does not feel the associated microstructure. In this paper, we inspect how to go beyond this limitation. This is done by "re-introducing" as incident waves the waves that have been excited in the near field of the perforated layer. Next the transmission spectrum is reinterpreted in view of two ingredients. (i) In the low-frequency regime, we use the transmission spectrum of the actual incident wave, and this reduces to the scholar exercise of the reflection and transmission of a homogeneous birefringent layer. (ii) Next, the same exercise is proposed, but considering incident evanescent waves. The role of these waves are negligible in general, *except* if they become resonant. This occurs at the cut-off frequencies, leading to the aforementioned extinctions observed by Wood for gratings, and we denote them destructive resonances (DR). Also, below the cut-off frequencies, an enhancement in the transmission is observed. This enhancement corresponds to resonances of guided waves (we call them constructive resonances, CR), equivalent to spoof plasmons. The dispersion relations of these resonant waves are derived in the equivalent birefringent layer, revealing their place in the spectrum, and the crucial role that they play in the transmission properties of the perforated layer. We end with promising perspectives to extend the homogenization process to a two-coupled-wave analysis.

2. Classical homogenization

We consider a layer of sound hard material of thickness ℓ perforated with thin slits of width w periodically located with spacing h (and the filling fraction of air $\varphi = w/h$ is small, $\varphi = 0.1$ in the following). The incident wave with wavenumber k hits the array with incidence angle θ (Fig. 1(a)).

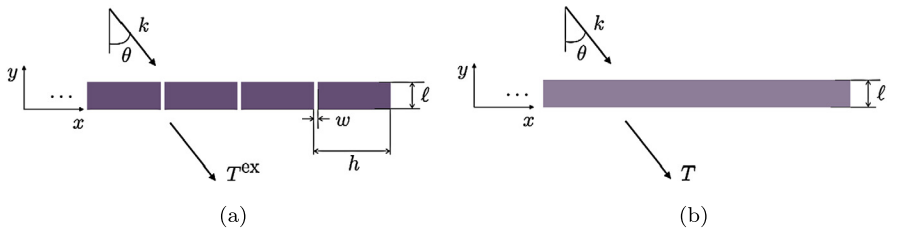

Fig. 1. (Color online.) (a) Geometry of the perforated sound hard layer. The filling fraction of the air is $\varphi = w/h$ ($\varphi = 0.1$ will be considered). (b) Equivalent birefringent layer.

When solving the exact problem, the reflected and transmitted pressure fields read

$$\begin{cases} p^{ex}(x,\, y \geq \ell) = e^{i\beta x}\left[e^{-i\sqrt{k^2-\beta^2}\,y} + R^{ex}\, e^{i\sqrt{k^2-\beta^2}\,y}\right] + \displaystyle\sum_{n\neq 0} R_n^{ex}\, e^{i(\beta+2n\pi/h)x}\, e^{i\sqrt{k^2-(\beta+2n\pi/h)^2}\,y}, \\ p^{ex}(x,\, y \leq 0) = T^{ex}\, e^{i\beta x} e^{-i\sqrt{k^2-\beta^2}\,y} + \displaystyle\sum_{n\neq 0} T_n^{ex}\, e^{i(\beta+2n\pi/h)x}\, e^{-i\sqrt{k^2-(\beta+2n\pi/h)^2}\,y} \end{cases} \tag{1}$$

with $\beta = k\sin\theta$ the component of the incident wavenumber along x. (R^{ex}, T^{ex}) and (R_n^{ex}, T_n^{ex}) are the reflection and transmission coefficients of, respectively, the incident wave and the waves generated in the near field of the array. These waves are propagating for $k > k_n^c$, evanescent otherwise, with k_n^c their cut-off frequencies:

$$\begin{cases} k_n^c = 2n\pi/(1-\sin\theta), & \text{if } n > 0, \\ k_n^c = -2n\pi/(1+\sin\theta), & \text{if } n < 0 \end{cases} \tag{2}$$

In the following, we refer to the "exact" solution $p^{ex}(x, y)$, the solution computed numerically using a modal method [13]. It is our goal to inspect whether or not the homogenized version of this array (Fig. 1(b)) is able to restitute the characteristics of the transmission spectrum T^{ex}. To do that, we will inspect two situations, where we consider $kh \in [0; 4\pi]$ with $\varphi = w/h = 0.1$ and

(i) the thickness $\ell = 0.3h$ is kept constant, and we consider varying incidence angles θ (thus, 1 to 4 waves are propagating),
(ii) the wave is sent at normal incidence $\theta = 0$ and we change the length of the slab $\ell/h \in [0.1, 2]$ (leading to 1 or 2 propagating waves).

2.1. Classical homogenization: from a perforated sound hard layer toward an effective birefringent layer

The homogenization theory of layered medium allows us to determine the effective properties of the equivalent homogeneous layer [17,18]. First, the wave equation in the succession of sound hard layers and thin air slits can be written:

$$\nabla\cdot\left[\frac{1}{\rho(x,y)}\nabla p(x,y)\right] + \frac{k^2}{B(x,y)}p(x,y) = 0 \tag{3}$$

with $1/\rho(x, y) = 1/B(x, y) \to 0$ in the sound hard material and $\rho = B = 1$ in the air. Omitting the finite size of the array $0 \leq y \leq \ell$, the medium is simply layered with $\rho(x)$ and $B(x)$, and the wave equation reads:

$$\frac{\partial}{\partial x}\left[\frac{1}{\rho(x)}\frac{\partial}{\partial x}p(x,y)\right] + \frac{1}{\rho(x)}\frac{\partial^2}{\partial y^2}p(x,y) + \frac{k^2}{B(x)}p(x,y) = 0 \tag{4}$$

Owing to the homogenization theory of layered media, this medium is shown to be equivalent, at dominant order, to an effective birefringent medium with extraordinary index $n_e^2 = \rho_e/\overline{B}$ (and $\rho_e = \langle\rho\rangle$, $\overline{B} = \langle 1/B\rangle^{-1}$) along x and ordinary index $n_o^2 = \rho_o/\overline{B}$ (with $\rho_o = \langle 1/\rho\rangle^{-1}$) along y.

$$\frac{1}{\rho_e}\frac{\partial^2}{\partial x^2}p(x,y) + \frac{1}{\rho_o}\frac{\partial^2}{\partial y^2}p(x,y) + \frac{k^2}{\overline{B}}p(x,y) = 0 \tag{5}$$

φ being the filling fraction of the air within the structure, we have $\rho_e = (1-\varphi)\rho_{SH} \to \infty$ (ρ_{SH} denotes the mass density of the sound hard material), $\rho_o = 1/\varphi$ and $\overline{B} = 1/\varphi$, leading to the refractive indices

$$n_e^2 = \varphi(1-\varphi)\rho_{SH}, \quad n_o^2 = 1 \tag{6}$$

In our analysis, ρ_{SH} is large (typically 10^3 for usual metals) and φ is small, thus *a priori* n_e^2 is large because of the sound hard materials, but this can be compensated by the small thickness of the slits. This case is disregarded, and we consider in

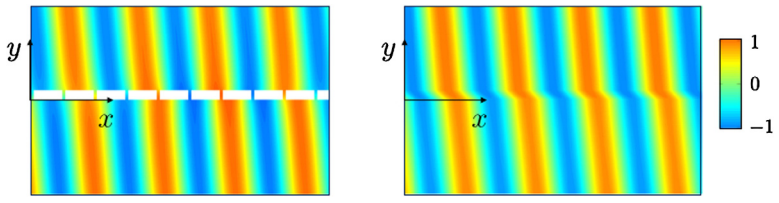

(a) $p^{\mathrm{ex}}(x,y)$ (b) $p(x,y)$

Fig. 2. (Color online.) Real part of the pressure fields, (a) $p^{\mathrm{ex}}(x,y)$ and (b) $p(x,y)$ for $\varphi=0.1$, $\ell=0.3h$, $kh=0.9\pi$ and $\theta=85°$, close to the Brewster angle $\theta_{\mathrm{B}}=\cos^{-1}\varphi$ realizing impedance matching in the homogenized problem.

the following $1/n_{\mathrm{e}}\to 0$. Next, we consider the incident wave of the actual problem. The solution for the pressure $p(x,y)$ in the birefringent layer reads

$$\begin{cases} p(x,y\geq\ell)=\mathrm{e}^{\mathrm{i}\beta x}\left[\mathrm{e}^{-\mathrm{i}\sqrt{k^2-\beta^2}\,y}+R\,\mathrm{e}^{\mathrm{i}\sqrt{k^2-\beta^2}\,y}\right],\\ p(x,0\geq y<\ell)=\mathrm{e}^{\mathrm{i}\beta x}\left[A\,\mathrm{e}^{-\mathrm{i}\kappa y}+B\,\mathrm{e}^{-\mathrm{i}\kappa y}\right],\\ p(x,y<0)=T\,\mathrm{e}^{\mathrm{i}\beta x}\,\mathrm{e}^{-\mathrm{i}\sqrt{k^2-\beta^2}\,y}\end{cases} \tag{7}$$

with $\kappa=n_{\mathrm{o}}\sqrt{k^2-\beta^2/n_{\mathrm{e}}^2}$ the component along y of the wavenumber inside the layer. In the present case, $\kappa\simeq k$, and the impedance ratio takes the form

$$\xi=\frac{\sqrt{k^2-\beta^2}}{\varphi\,k} \tag{8}$$

The layer being homogeneous, it is a simple exercise to calculate R, T and (A,B). The result for T is

$$T=\frac{\xi(1+t^2)}{\xi(1-t^2)-\mathrm{i}(1+\xi^2)t} \tag{9}$$

with $t\equiv\tan k\ell/2$. It follows that perfect transmissions are obtained for

$$\begin{cases}\xi=1,\ \text{realizing the condition of perfect impedance matching,}\\ k\ell=n\pi,\ \text{corresponding to } t=0,\infty,\ \text{(Fabry–Pérot, FP, resonances)}\end{cases} \tag{10}$$

(for the former relation, we used $1-t^2-2it=(1+t^2)\,\mathrm{e}^{-\mathrm{i}k\ell}$).

2.2. Validity of the homogenization predictions

We inspect the validity of the predictions for perfect transmissions in Eqs. (10). The first condition of impedance matching $\xi=1$ can be obtained for a Brewster angle θ_{B}, as first pointed out by [14] and popularized by Alù and co-workers in a series of papers (see, *e.g.*, [15]):

$$\theta_{\mathrm{B}}=\cos^{-1}\varphi \tag{11}$$

In a previous paper [16], we have already shown the validity of the classical homogenization to derive the Brewster angle for any sort of arrays, sound penetrable or not, and including structural effects. This is confirmed here in Fig. 2, where we reported the real part of pressure fields $p^{\mathrm{ex}}(x,y)$ (exact) and $p(x,y)$ (of the homogenized problem) for $\ell=0.3h$, $kh=0.9\pi$ and $\theta=85°$ close to $\theta_{\mathrm{B}}\simeq 84.26°$.

Next, the condition of FP resonances, $k\ell=n\pi$ is regarded. Fig. 3 reports the real part of the pressure fields $p(x,y)$ for $k\ell=\pi,2\pi$ and 3π for normal incidence $\theta=0$ and $\ell=1.5h$ (bottom panel). At these frequencies, the exact pressure fields $p^{\mathrm{ex}}(x,y)$ do not experience perfect transmission (the results are not reported). We find perfect transmissions for significantly shifted frequencies $k\ell=0.9\pi$, 1.8π and 2.7π (top panel).

In addition to the shifts in the frequencies realizing perfect transmission, we clearly observe in the pattern of p^{ex} high amplitudes of the evanescent waves in the near field, which are not accounted for in the homogenized problem, and we can think that such a large amplitude in the evanescent field is not incidental. To better understand these net discrepancies, we report in Fig. 4 the whole spectra T^{ex} to be compared with the spectra T of the homogenized problem, in the (θ,kh) plane for $\ell=0.3h$ (case (i), Fig. 4(a)), and in the $(\ell/h,kh)$ plane for $\theta=0$ (case (ii), Fig. 4(a)).

As expected, above the first cut-off frequency ($k^{\mathrm{c}}_{-1}=2\pi/(1+\sin\theta)$ in (i) and $k^{\mathrm{c}}_{1}=2\pi$ in (ii)), the homogenized version of the perforated layer is not able to describe the complexity of the transmission spectrum T^{ex}. The cut-off frequencies produce a complete extinction or at least a net decrease in the transmission (DR in Fig. 5). These are the analogs for our array of the extinctions observed by Wood for a reflection grating. In the case (i), the first extinction at $kh=2\pi/(1+\sin\theta)\simeq 1.22\pi$

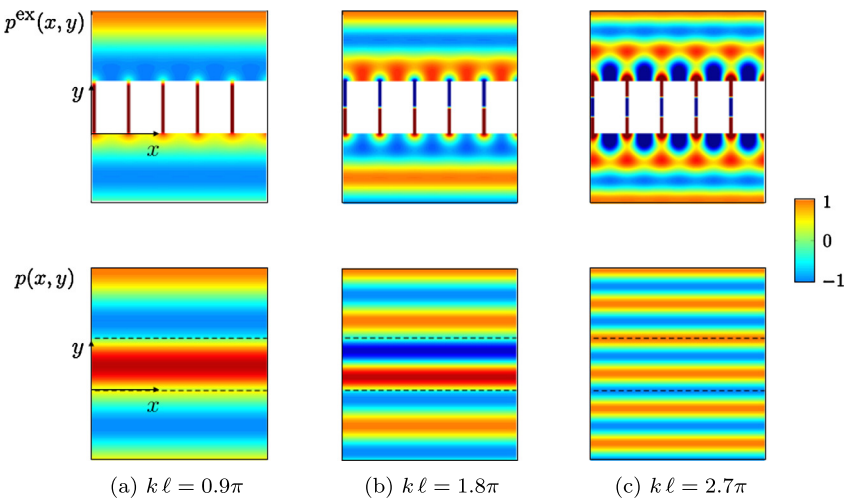

Fig. 3. (Color online.) Real part of the pressure fields $p^{ex}(x, y)$ realizing perfect transmission at $k\ell = 0.9\pi$, 1.8π and 2.7π for $\theta = 0$ and $\ell = 1.5h$. These perfect transmissions are significantly shifted from the FP predicted in the homogenized problem for $k\ell = \pi, 2\pi$ and 3π (pressure fields $p(x, y)$ are reported on the bottom).

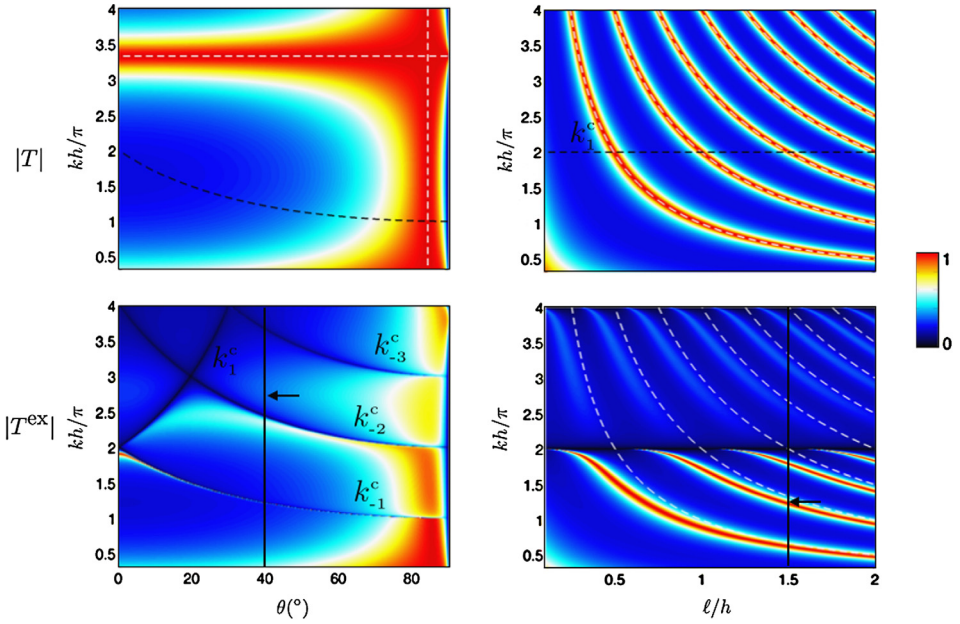

Fig. 4. (Color online.) Transmission spectra $|T|$ of the birefringent layer, Eq. (9), and $|T^{ex}|$ of the perforated sound hard layer, in the (θ, kh) plane for $\ell = 0.3h$ (case (i)) and in the $(\ell/h, kh)$ plane for $\theta = 0$ (case (ii)). The dotted white lines indicate the FP resonances and Brewster angle predicted within classical homogenization. Dotted black lines indicate the cut-off frequencies. Plain black lines with arrow are the lines corresponding to the profiles in Fig. 5.

in Fig. 5(a) is a typical max–min Fano resonance occurring within a variation of kh of order 10^{-3}, as reported by Wood: "Drop from maximum illumination to minimum [...] occurred within a range of wavelengths not greater than the distance between two sodium lines." The vicinity of a maximum transmission and a minimum transmission is not automatic. If the minima are always associated with the resonance of a wave passing through its cut-off frequency (we call them destructive resonance DR), we will see that all the local maxima are attributable to a resonance in the evanescent field, independently of the DR-frequencies (and we call them constructive interferences, CR). Besides, the CR maxima are not so closely related to the FP condition predicted within classical homogenization. This is clear in the case (i), where the FP, being predicted above the first cut-off frequency, does not leave any trace on the actual spectrum of T^{ex}, and it is replaced by other maxima. Also, and as previously reported in Fig. 3, the perfect transmissions below the first cut-off frequency $kh = 2\pi$ in the case (ii) do

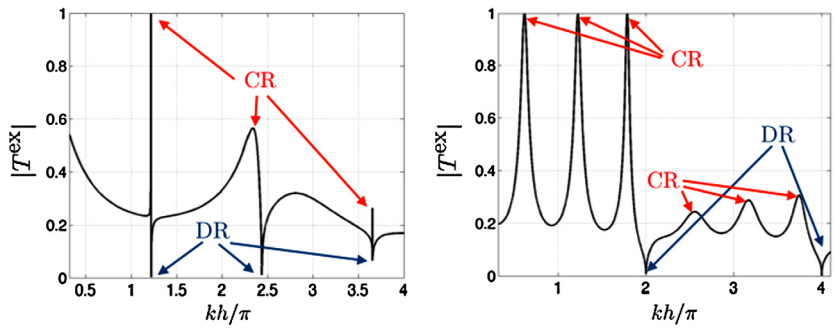

(a) $\theta = 40°$ (b) $\ell/h = 1.5$

Fig. 5. (Color online.) Transmission $|T^{ex}|$ as a function of k along the two vertical lines (with arrow) in Fig. 4.

not coincide with the FP. It is our goal now to understand this behavior, in view of possible resonances of the evanescent field in our homogenized problem.

3. Homogenization of the evanescent field

As previously said, the plane wave incident on the perforated layer produces many evanescent waves, and possibly propagating ones. In the homogenized problem, the layer, being homogeneous, does not produce wave coupling, and we have to restore the information of this near field. This can be done by considering that the incident field in the homogenized problem is composed of all these waves. For each one, we can define a scattering problem

$$\begin{cases} p_n(x, y \geq \ell) = \mathrm{e}^{\mathrm{i}\beta_n x}\left[\mathrm{e}^{-\mathrm{i}\sqrt{k^2-\beta_n^2}\,y} + R_n\,\mathrm{e}^{\mathrm{i}\sqrt{k^2-\beta_n)^2}\,y}\right], \\ p_n(x, 0 \geq y < \ell) = \mathrm{e}^{\mathrm{i}\beta_n x}\left[A_n\,\mathrm{e}^{-\mathrm{i}\kappa_n y} + B_n\,\mathrm{e}^{-\mathrm{i}\kappa_n y}\right], \\ p_n(x, y \leq 0) = T_n\,\mathrm{e}^{\mathrm{i}\beta_n x}\,\mathrm{e}^{-\mathrm{i}\sqrt{k^2-\beta_n)^2}\,y} \end{cases} \tag{12}$$

with $\beta_n = k\sin\theta + 2n\pi/h$. Thus, the formalism used previously for the incident plane wave can be applied to any of the evanescent waves. These waves do not transport energy and they are exponentially decreasing when moving away from the interfaces $y = 0, \ell$. Thus, we expect them to produce an effect on the incident wave only if their amplitude becomes large, that is, in the case of resonances. This means that we are now looking at divergences of R_n and T_n, and T_n is given by

$$T_n = \frac{\xi_n(1+t^2)}{\xi_n(1-t^2) - \mathrm{i}\,(1+\xi_n^2)\,t} \tag{13}$$

with

$$\xi_n = \frac{\sqrt{k^2 - (\beta + 2n\pi/h)^2}}{k\varphi} \tag{14}$$

Owing to the identity $\xi_n(1-t^2) - \mathrm{i}\,(1+\xi_n^2)t = -\mathrm{i}\,t\,(\xi_n - \mathrm{i}\,t)(\xi_n + \mathrm{i}/t)$, this condition $1/|T_n| = 0$ becomes:

$$\text{dispersion relation of guided waves} \quad \begin{cases} k^2 - (\beta + 2n\pi/h)^2 = -k^2\varphi^2\tan^2 k\,\ell/2, & \text{if } \tan k\,\ell/2 > 0, \\ k^2 - (\beta + 2n\pi/h)^2 = -\frac{k^2\varphi^2}{\tan^2 k\,\ell/2}, & \text{if } \tan k\,\ell/2 < 0 \end{cases} \tag{15}$$

This dispersion relation corresponds to resonances of guided waves within the birefringent layer, that is waves that propagate in the birefringent layer with wavenumber β (along x) and that are evanescent in the air. Indeed, the resonance predicted by the dispersion relation above occurs at frequency k such as $k^2 - (\beta + 2n\pi/h) < 0$, that is below the cut-off frequency. In other words, this is the equivalent for an array of the dispersion relation of spoof plasmons in gratings.

To inspect whether or not the resonances in the homogenized problem have a counterpart in the real problem, we report them on the transmission spectra T^{ex} in Fig. 6. To be more explicit, let us consider in more details our cases (i) and (ii). In the case (i), the length ℓ is constant and θ varies; in the present case, with $\ell/h = 0.3$ nd $kh \in [0, 4\pi]$, the $\tan k\,\ell/2$ is positive until $kh \simeq 3.3\pi$, and we inspect this range only. Thus, only the first branch in Eq. (15) is regarded. Explicit dispersion relations read

$$\text{dispersion relation, case (i)} \quad \begin{cases} \theta = \sin^{-1}\left[-\frac{2n\pi}{kh} - \sqrt{1 + \varphi^2\tan k\,\ell/2)^2)}\right], & \text{for } n = -1, -2, -3, \\ \theta = \sin^{-1}\left[-\frac{2n\pi}{kh} + \sqrt{1 + \varphi^2\tan k\,\ell/2)^2)}\right], & \text{for } n = 1 \end{cases} \tag{16}$$

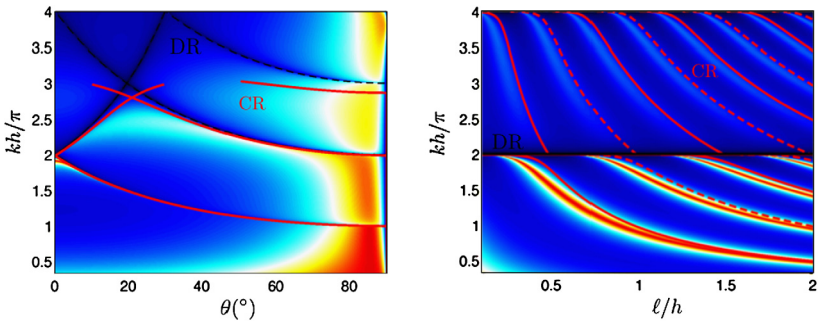

(a) Case (i) (b) Case (ii)

Fig. 6. (Color online.) Same spectra as in Fig. 4. The red lines show the dispersion relation of the resonant guided waves (CR) in the homogenized problem, Eq. (15) [see also Eq. (16) for the case (i) and Eq. (17) for the case (ii)]. In case (ii), plain lines refer to ℓ_1 and dotted lines to ℓ_2 in Eq. (17). Dotted black lines are the cut-off frequencies (DR).

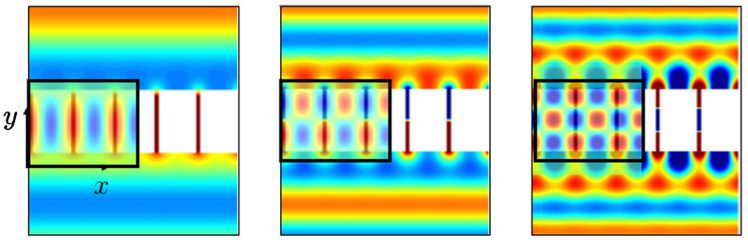

Fig. 7. (Color online.) Case (ii). Real part of the pressure fields at the CR, see caption of Fig. 3. The insets show the real part of the pressure field $p_1(x, y)$, Eq. (12), for the resonant guided waves of the homogenized problem, Eqs. (17).

In the case (ii), $\theta = 0$ and ℓ varies. Here, the two branches in Eq. (15) exist for $n = 1$ and $n = 2$, and each branch gives multiple resonances (with index m) because of the multivaluation of the function tan. We get

$$\text{dispersion relation, case (ii)} \begin{cases} \ell_1 = \frac{2}{k}\left[m\pi + \tan^{-1}\frac{\sqrt{(2n\pi/kh)^2-1}}{\varphi}\right], & \text{for } \tan k\ell/2 > 0, \\ \ell_2 = \frac{2}{k}\left[m\pi - \tan^{-1}\frac{\varphi}{\sqrt{(2n\pi/kh)^2-1}}\right], & \text{for } \tan k\ell/2 < 0 \end{cases} \tag{17}$$

and we observe $m = 1, 2$ for $n = 1$ and $m = 1, 2, 3, 4$ for $n = 2$. The agreement is rather good between the perfect, or enhanced, transmissions and the place of the resonances of the guided waves in the homogenized problem. This indicates, when they are in competition (as in the case (ii)), that the resonances of the guided modes dominate the transmission of the incident wave, and they outweigh the FP resonances.

We now end our inspection of the physical meaning of the guided mode in the birefringent layer by considering two aspects. First, we come back to the pressure fields $p^{\text{ex}}(x, y)$ in Fig. 3, which were found not so well described by the FP of the classical homogenization; these are the three perfect transmissions occurring at $kh < 2\pi$ in Fig. 5(b). We already observed that the near field was of large amplitude at these perfect transmissions. We report in Fig. 7 the exact pressure fields, but now we insert the pressure field $p_1(x, y)$, Eq. (12), at the resonances of the guided mode, Eqs. (17). The frequencies of the CR ($kh = 0.6\pi$, 1.2π, and 1.8π) are now much closer to the frequencies of the guided modes in the homogenized problem: $kh = 0.6\pi$, 1.3π and 1.9π, and the guided waves mimic well the resonant first evanescent wave in the slits (also visible in the near field).

Our last inspection concerns the behavior of an evanescent waves in the real problem and its interaction with the incident wave. To do that, we compute the solution to the real problem, Eq. (1), but accounting only for the incident wave and one evanescent wave. Thus, the result describes the behavior of the real evanescent wave in the near field but it omits the interaction with the other evanescent waves, and with the other propagating waves (if any). The transmission spectra T_n^{ex}, defined in Eq. (1), are reported in Fig. 8 in the cases (i) and (ii), and we have added for each value of n the dispersion relations of the guided modes in the corresponding homogenized problem. The result is now excellent, with no shifts between the high values of the evanescent waves in the real problem and the resonances of the guided waves. This suggests that the small shifts previously observed in Fig. 6 between the high transmissions of the incident wave and the resonances of the guided waves were attributable to more complex wave coupling rather than to our approximation of homogenized medium.

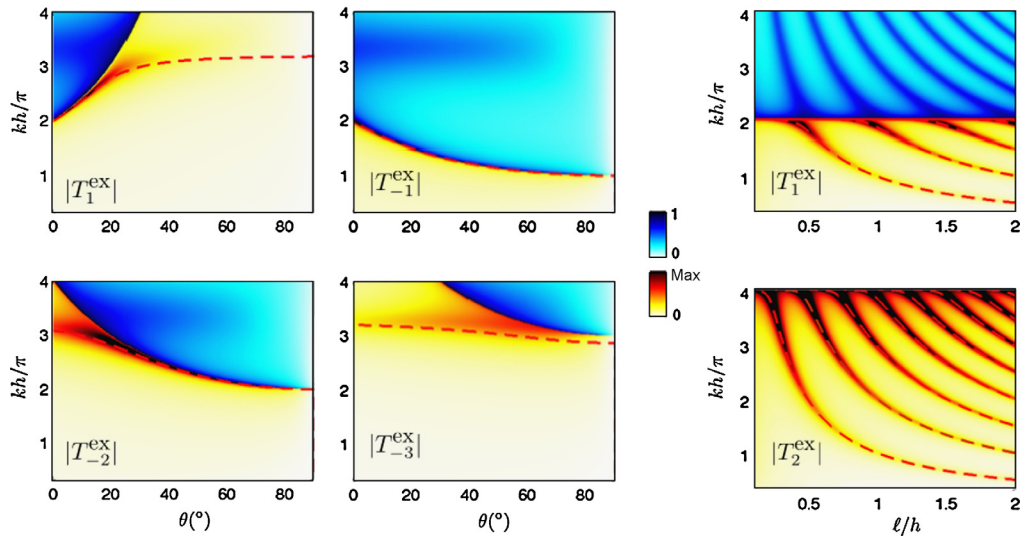

(a) Case (i) (b) Case (ii)

Fig. 8. (Color online.) Transmission spectra $|T_n^{\rm ex}|$ of the waves excited in the near field of the perforated layer (two different color maps are used to distinguish the character evanescent or propagating of the wave) when taking into account only the incident wave and one wave with index n in Eq. (1). The dotted red lines show the dispersion relation of the guided waves in the homogenized problem, Eqs. (15) (or Eqs. (16)–(17)).

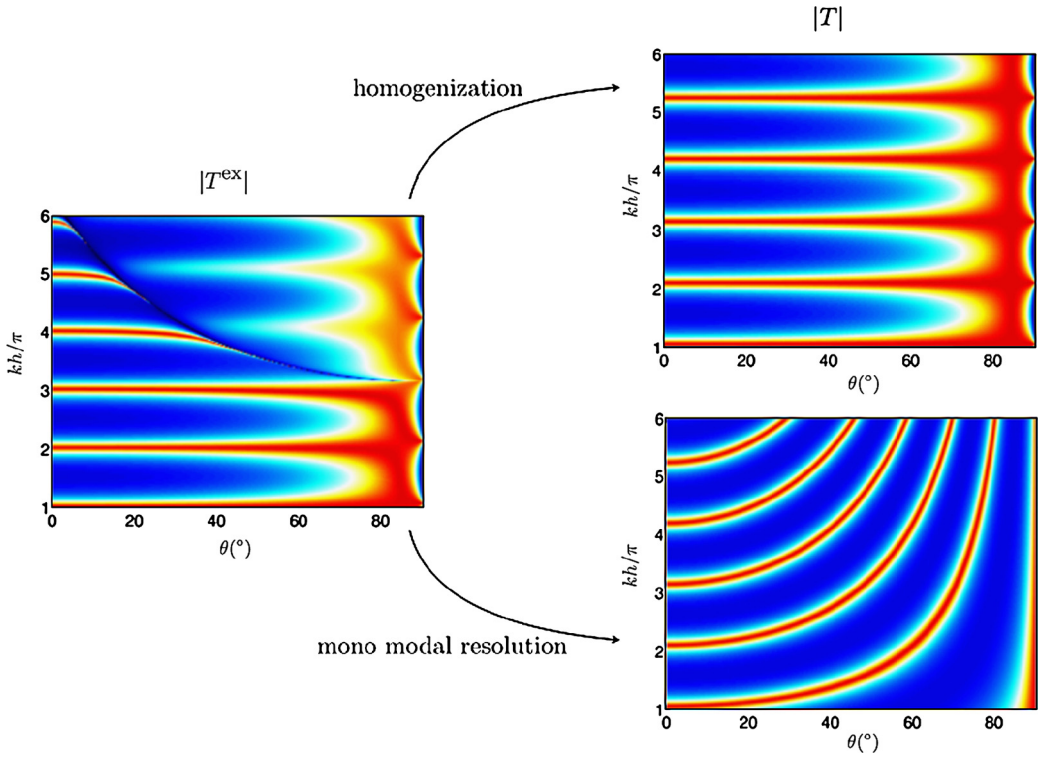

Fig. 9. (Color online.) Comparison between the converged spectrum $|T^{\rm ex}|$ in the case (i) with $\ell/h = 3$ and: on the top-right, the spectrum obtained using classical homogenization, on the bottom-right the spectrum coming from the a mono modal numerical calculation.

4. Concluding remarks

We have shown that the use of homogenization theory can be helpful to analyze the complex transmission spectra through a perforated sound hard layer, well beyond the usual low-frequency regime. By analyzing the possible resonances of the evanescent waves excited in the near field, it is possible to derive precise dispersion relations by considering the

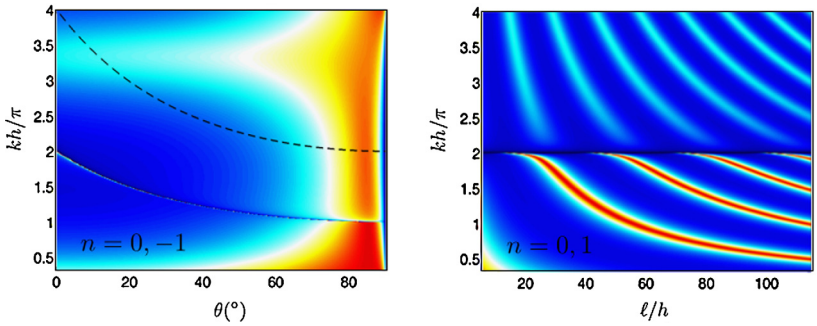

(a) Case (i) (b) Case (ii)

Fig. 10. (Color online.) Transmission spectra in cases (i) and (ii) calculated numerically accounting for the incident wave and the first wave passing through its cut-off frequency.

waves guided within the equivalent birefringent layer in the homogenized problem. To make a step further, we conclude with one remark and one perspective that are related.

First, we report in Fig. 9 the spectrum obtained using our numerical calculation but omitting the evanescent field in Eq. (1), and thus accounting for the incident wave only (mono modal approximation) and the spectrum obtained using classical homogenization, where only the incident wave is regarded, but in the homogenized problem. The converged spectrum T^{ex} is given for comparison. To build these spectra, we have considered the case (i), but with $\ell/h = 3$ in order to get FP in the low-frequency regime. Obviously, the mono modal approximation is unable to describe the transmission spectra, even in the low-frequency regime (it misses notably the Brewster angle and captures the FP only at normal incidence). To the opposite, the classical homogenization allows to properly describe the low-frequency regime; note that similar conclusions on the effect of CR and DR could be drawn but they are less marked in this case.

Next, we report in Fig. 10 the spectra obtained in the cases (i) and (ii), which have been the subjects of the present study. There, the spectra have been calculated numerically taking into account the incident wave and the first wave passing through its cut-off frequency. The improvement is quite clear. Owing to the previous remark that the classical homogenization problem allows one to better restitute the transmission properties than the mono modal approach, an extension of the homogenization to a two-coupled-wave problem sounds promising. Works are in progress in this direction.

References

[1] R.W. Wood, On a remarkable case of uneven distribution of light in a diffraction grating spectrum, Philos. Mag. 4 (1902) 396–402.
[2] Rayleigh, Note on the remarkable case of diffraction spectra described by prof. Wood, Philos. Mag. 1 (4) (1907) 60–65.
[3] A. Hessel, A.A. Oliner, A new theory of Wood's anomalies on optical gratings, Appl. Opt. 4 (1965) 1275–1297.
[4] D. Maystre, Theory of Wood's Anomalies, Plasmonics, vol. 167, Springer-Verlag, Berlin, Heidelberg, 2012, pp. 39–83.
[5] F.J. Garcia-Vidal, L. Martín-Moreno, J.B. Pendry, Surfaces with holes in them: new plasmonic metamaterials, J. Opt. A, Pure Appl. Opt. 7 (2005) S97–S101.
[6] J. Zhu, Y. Chen, X. Zhu, F.J. Garcia-Vidal, S. Yin, W. Zhang, X. Zhang, Acoustic rainbow trapping, Sci. Rep. 3 (2011) 1728.
[7] F. Lemoult, N. Kaina, M. Fink, G. Lerosey, Wave propagation control at the deep subwavelength scale in metamaterials, Nat. Phys. 9 (2013) 55–60.
[8] L. Kelders, J.-F. Allard, W. Lauriks, Ultrasonic surface waves above rectangular-groove gratings, J. Acoust. Soc. Amer. 103 (5) (1998) 2730–2733.
[9] E. Popov, S. Enoch, Mystery of the double limit in homogenization of finitely or perfectly conducting periodic structures, Opt. Lett. 32 (23) (2007) 3441–3443.
[10] D. Felbacq, G. Bouchitté, Homogenization of a set of parallel fibres, Waves Random Media 7 (2) (1997) 245–256.
[11] J.T. Shen, Peter B. Catrysse, Shanhui Fan, Mechanism for designing metallic metamaterials with a high index of refraction, Phys. Rev. Lett. 94 (2005) 197401.
[12] J. Shin, J.T. Shen, P.B. Catrysse, S. Fan, Cut-through metal slit array as an anisotropic metamaterial film, IEEE J. Sel. Top. Quantum Electron. 12 (6) (2006) 1116–1122.
[13] A. Maurel, J.-F. Mercier, S. Félix, Wave propagation through penetrable scatterers in a waveguide and through a penetrable grating, J. Amer. Soc. Acoust. 135 (1) (2013) 165–174.
[14] X.-R. Huang, R.-W. Peng, R.-H. Fan, Making metals transparent for white light by spoof surface plasmons, Phys. Rev. Lett. 105 (2010) 243901.
[15] A. Alù, G. D'Aguanno, N. Mattiucci, M.J. Bloemer, Plasmonic Brewster angle: broadband extraordinary transmission through optical gratings, Phys. Rev. Lett. 106 (12) (2011) 123902.
[16] A. Maurel, S. Félix, J.-F. Mercier, Enhanced transmission through gratings: structural and geometrical effects, Phys. Rev. B 88 (2013) 115416.
[17] D. Cioranescu, P. Donato, An Introduction to Homogenization, vol. 8, Oxford University Press, Oxford, UK, 1999.
[18] A. Bensoussan, J.-L. Lions, G. Papanicolaou, Asymptotic Analysis for Periodic Structures, vol. 374, American Mathematical Society, 2011.